1-1-2015

Further studies on the relationship between IRSL and BLSL at relatively high temperatures for potassium-feldspar from sediments

Zhijun Gong
University of Hong Kong

Bo Li
University of Wollongong, bli@uow.edu.au

Sheng-Hua Li
University of Hong Kong, shli@hku.hk

Further studies on the relationship between IRSL and BLSL at relatively high temperatures for potassium-feldspar from sediments

Abstract

In optical dating of potassium-feldspar, the luminescence signals can be stimulated by both infrared (IR) light and blue light (BL). To develop reliable dating methods using different stimulation light sources for feldspars, it is important to understand the sources of the traps associated with the infrared stimulated luminescence (IRSL) and blue light stimulated luminescence (BLSL) and their relationship. In this study, we explored the luminescence characteristics of IRSL and BLSL at different stimulation temperatures (from 60 °C to 200 °C) and their relationship based on five sets of experiments, i.e. post-IR BLSL, post-BL IRSL experiments, pulse annealing test, dose-response test and laboratory fading rate test. Our results suggest that the luminescence characteristics of IRSL and BLSL and their relationship are dependent on stimulation temperature. For IR stimulation at a relatively high temperature of 200 °C, at least two components of IRSL signals are involved in the process. One component of IRSL signals can be easily bleached by BL stimulation at 60 °C, while the other is relatively hard to be bleached by BL stimulation at 60 °C. The two components have different luminescence properties, such as thermal stability, dose-response and laboratory fading rate.

Disciplines

Medicine and Health Sciences | Social and Behavioral Sciences

Publication Details

Gong, Z., Li, B. & Li, S. (2015). Further studies on the relationship between IRSL and BLSL at relatively high temperatures for potassium-feldspar from sediments. Journal of Luminescence, 159 238-245.

Further studies on the relationship between IRSL and BLSL at relatively high temperatures for potassium-feldspar from sediments

Zhijun Gong[a,b], Bo Li[a,c], Sheng-Hua Li[a,*]

[a] Department of Earth Sciences, The University of Hong Kong, Pokfulam Road, Hong Kong, China

[b] Key laboratory of Cenozoic Geology and Environment, Institute of Geology and Geophysics, Chinese Academy of Sciences, Beijing, China

[c] Centre for Archaeological Science, School of Earth and Environmental Sciences, University of Wollongong, Wollongong, NSW 2522, Australia

*Corresponding author: shli@hku.hk

Abstract:

In optical dating of potassium-feldspar, the luminescence signals can be stimulated by both infrared (IR) light and blue light (BL). To develop reliable dating methods using different stimulation light sources for feldspars, it is important to understand the sources of the traps associated with the infrared stimulated luminescence (IRSL) and blue light stimulated luminescence (BLSL) and their relationship. In this study, we explored the luminescence characteristics of IRSL and BLSL at different stimulation temperatures (from 60 °C to 200 °C) and their relationship based on five sets of experiments, i.e. post-IR BLSL, post-BL IRSL experiments, pulse annealing test, dose response test and laboratory fading rate test. Our results suggest that the luminescence characteristics of IRSL and BLSL and their relationship are dependent on stimulation temperature. For IR stimulation at a relatively high temperature of 200 °C, at least two components of IRSL signals are involved in the process. One component of IRSL signals can be easily bleached by BL stimulation at 60 °C, while the other is relatively hard to be bleached by BL stimulation at 60 °C. The two components have different luminescence properties, such as thermal stability, dose response and laboratory fading rate.

Keywords: K-feldspar, IRSL, BLSL, component

---

1. Introduction

Both quartz and potassium-rich feldspar (K-feldspar) have been widely used as natural dosimeters for optically stimulated luminescence (OSL) dating (Aitken, 1998). Compared with quartz OSL, the infrared stimulated luminescence (IRSL) signal from K-feldspar (Hütt et al., 1988) has advantages of much brighter luminescence signals and much higher dose saturation level, making feldspar as an attractive candidate for luminescene dating of the natural sedimentary samples. However, the usage of K-feldspar for dating has long been hindered by the anomalous fading of the trapped charges related to the IRSL signals (e.g. Spooner, 1994; Huntley and Lamonthe, 2001; Li and Li, 2008).

More recently, progress in understanding anomalous fading in feldspar has raised the prospect of isolating a non-fading component from the IRSL at relatively high temperatures (Thomsen et al., 2008; Li, 2010; Jain and Ankjærgaard, 2011; Li and Li, 2013). Correspondingly, a two-step post IR IRSL (pIRIR) protocol (Buylaert et al., 2009; Thiel et al., 2011) and a multi-elevated-temperature post-IR IRSL (MET-pIRIR) protocol (Li and Li, 2011a) have been proposed to overcome anomalous fading for dating K-feldspar from sediments, which offer the promising potential for extending the luminescence dating limit (Thiel et al., 2011; Li and Li, 2012; Li et al., 2013, 2014a). However, the high temperature pIRIR signal (e.g. >200 °C) is found to be more difficult to bleach than the IRSL signal measured at lower temperatures (Li and Li, 2011a; Buylaert et al., 2012; Murray et al., 2012), and it usually requires up to several hours or even days of exposure to sunlight or a solar simulator to bleach the pIRIR signal down to a stable level (here the term "bleach" means to reduce the luminescence intensity by optical stimulation). For some samples, a significant non-bleachable (or residual) component in the pIRIR signals was left even after a prolonged bleaching period using solar simulator or sunlight (Buylaert et al., 2011; Lowick et al., 2012; Chen et al., 2013; Li et al., 2014b). These studies suggest that the IRSL signals recorded at relatively high temperature have different luminescence behavior compared with the IRSL signals at room temperature.

There have been several studies conducted to explore the relationship between luminescence with IR stimulation and luminescence with visible wavelength light stimulation. It was demonstrated that the majority of green light stimulated luminescence (GLSL) can be bleached by prolonged IR light and an upper limit of ～ 90% GLSL was depleted as a result of IR bleaching at room temperature (Duller and Bøtter-Jensen, 1993; Galloway, 1994). Jain and Singhvi (2001) concluded that the blue-green (BG) stimulated luminescence measured at 125 °C is associated with at least two trap populations. One trap population is responsive to both IR stimulation and BG stimulation. Another trap population is only responsive to BG stimulation. Gong et al. (2012) conducted a study on the relationship between the infrared stimulated luminescence (IRSL) and blue light stimulated luminescence (BLSL) at 60 °C. They observed that most of the IRSL signals at 60 °C can be bleached by BL at 60 °C, while the BLSL signals at 60 °C can only be partially bleached by IR at 60 °C. The sources for the IRSL at 60 °C are mainly associated with the fast and medium components of the BLSL at 60 °C.

In this study, in order to better understand the sources of the traps associated with the IRSL and BLSL, we further explore the relationship between IRSL and BLSL using K-feldspar from two aeolian sand samples. The luminescence properties, in terms of thermal stability, dose response and laboratory fading rate, are also examined for the different IRSL components at a relatively high temperature of 200 °C.

2. Samples and equipment

Two aeolian sand samples (HSDK-11 and SY) from the Hunshandake desert in northeast China were used in this study. Both samples have been investigated in previous studies (Li et al., 2002; Gong et al., 2013). The samples are from the same environmental settings of the same region and have similar luminescence behaviors, so the experimental results obtained from them should be comparable. The samples were treated with 10 % hydrochloric acid (HCl) and 10 % hydrogen peroxide (H_2O_2) to remove carbonate and organic matter, respectively, in subdued red light in the Luminescence Dating Laboratory, the University of Hong Kong. Grains of 150-180 μm in diameter were obtained by dry sieving. The K-feldspar grains were separated with heavy liquids (2.58 g·cm^{-3}) and then etched for 40 min with diluted (10 %) hydrofluoric acid (HF) to clean the grains. HCl (10 %) was used again to dissolve any contaminating fluorides after etching before final rinsing and drying. K-feldspar grains were prepared by mounting the grains in a monolayer, on a 9.8 mm diameter aluminum disc with “Silkospay” silicone oil.

The luminescence measurements of the sample HSDK-11 were carried out with an automated Risø TL-DA-15 reader equipped with an IR LED array (880 nm, FWHM 40 nm) and a blue LED array (470 nm, FWHM 20 nm) in the Luminescence Dating Laboratory, the University of Hong Kong. The IR and BL stimulations deliver ~135 mW·cm^{-2} and ~50 mW·cm^{-2} at the sample position, respectively (Bøtter-Jensen et al., 2003). To keep our results comparable with those from Gong et al. (2012), 90% of the full power was used for stimulation in this study. Irradiations were carried out within the reader using a ^{90}Sr/^{90}Y beta source which delivered a dose rate of 0.0761 Gy·s^{-1} to K-feldspar on aluminum discs. The IRSL and the BLSL signals were both detected after passing through 7.5-mm-thick U-340 filters, which mainly pass light from 290 nm to 370 nm with peak transmission at ~340 nm (Li et al., 2007b). The experimental work on the other sample SY was performed in the Luminescence Dating Laboratory, Institute of Geology and Geophysics, Chinese Academy of Sciences. The luminescence measurements of the sample SY were carried out with an automated Risø TL/OSL reader (TL/OSL-DA-15) using the similar equipment setting. The ^{90}Sr/^{90}Y beta source in the equipment delivered a dose rate of 0.0837 Gy·s^{-1} to K-feldspar on aluminum discs.

3. Experimental details and results

3.1 The relationship between the IRSL and the BLSL at different stimulation temperatures

Two sets of experiments, namely post-IR BLSL (pIR-BLSL) and post-blue light

IRSL (pBL-IRSL), are conducted to investigate the relationship between the IRSL and the BLSL at different stimulation temperatures. For simplification, we describe the stimulation temperatures used in the prior IR and post-IR BLSL as pIR(T_1)-BLSL(T_2), where T_1 is the stimulation temperature used in the prior IR measurement and T_2 is the temperature used in post-IR BLSL measurement.

3.1.1 pIR-BLSL experiments

The pIR-BLSL experiments were carried out using the procedure listed in Table 1. Four aliquots of of K-feldspar grains HSDK-11 were firstly heated to 500 °C and then given a dose of 30.4 Gy. These aliquots were subsequently preheat at 280 °C for 10 s and then bleached using IR stimulation at a temperature of T_1 for different periods ranging from 0 to 5000 s. The pIR-BLSL signal (L_x) was then measured at a temperature of T_2. After that, a test dose of 15.2 Gy was applied and the induced BLSL signal (T_x) was measured following the same preheat to monitor sensitivity change for L_x. The signals for both L_x and T_x were calculated from the integrated photon counts in the first 1 s of stimulation, with subtraction of the instrumental background signal. The experiments are conducted at a set of different temperature combinations, i.e. pIR(60)-BLSL(60), pIR(100)-BLSL(60), pIR(150)-BLSL(60), pIR(200)-BLSL(60) and pIR(200)-BLSL(200), respectively.

The IR bleaching effects on the pIR-BLSL signal for different periods of time are shown in Fig. 1. It is observed that the IR bleaching at higher temperatures can deplete the BLSL at 60 °C at a faster rate than IR stimulation at lower temperatures. The BLSL at 60 °C was bleached to about 5 % of the initial intensity after IR bleaching at 200 °C for 5000 s. In comparison, the BLSL at 60 °C was bleached to about 15 % of the initial intensity after IR bleaching at 60 °C for 5000 s. If we increase the stimulation temperature in BLSL from 60 to 200 °C, i.e. pIR(200)-BLSL (200), the IR stimulation at 200 °C can bleach the most of the traps associated with the BLSL at 200 °C and only 6 % of the initial intensity of the BLSL at 200 °C was remaining after IR bleaching at 200 °C for 5000 s (Fig. 1). The results suggest that both the BLSL measured at 60 °C and the BLSL at 200 °C can only be partially bleached by prolonged (up to 5000 s) IR stimulation even at a relatively high temperature (i.e. 200 °C).

In our previous study (Gong et al., 2012), it was found that the BLSL signals measured at 60 °C for the K-feldspar from sample HSDK-11 can be described using three first-order exponential components, which are termed as fast (F), medium (M) and slow (S) components. Gong et al. (2012) demonstrated that the sources for the IRSL at 60 °C are mainly associated with the fast and medium components of the BLSL at 60 °C. To further demonstrate the relationship between IRSL signal at relatively high temperatures and BLSL at 60 °C, the residual BLSL at 60 °C after IR bleaching for different time from 0 s to 5000 s were then fitted using three OSL components. It is found that the pIR-BLSL signals can be well described by the three exponential functions (all $R^2 > 0.96$). The relative ratios of the decay rates of the components of BLSL at 60 °C, i.e. b_f/b_m and b_m/b_s, are calculated at 4.87±0.14 and 10.69±0.41, respectively (here the parameters of b_f, b_m and b_s refer to the decay rate of the fast, medium and slow components of BLSL at 60 °C, respectively). It is noted that the assumption of that the BLSL process is first-order may not be true. However, this will not influence our conclusion because it is the relationship between the different parts of BLSL (represented by the fast, medium and slow components) and IRSL that is crucial for our study, rather than whether these components are first-order or not. We, however, acknowledge that there may be some uncertainty associated with the fitting and some results demonstrated by Fig. 2 and Fig. 6 might be partially influenced if these components are not first-order.

Fig. 2a illustrates four representative pIR-BLSL signals, which are fitted into three components. The results of IR bleaching for the fast, medium and slow component of BLSL at 60 °C are shown in Fig. 2b. It is observed that the IR stimulation at 200 °C for 5000 s can deplete 99 % of the fast component, ~99 % of the medium component but only ~38 % of the slow component for the BLSL at 60 °C, while IR stimulation at 60 °C for 5000 s can only deplete ~97 % of fast component, ~91 % of medium component and ~12 % of slow component, respectively, for the BLSL at 60 °C. These results indicate that IRSL obtained at 200 °C involves more traps associated with hard-to-bleach components (i.e. the medium and slow components) of BLSL at 60 °C than does the IR stimulation at 60 °C. The results are consistent with previous studies that the IRSL signals at high temperatures (e.g. >200 °C) are relatively harder to bleach than the IRSL at 60 °C (Buylaert et al., 2011; Li and Li, 2011a; Chen et al., 2013).

The relationship between the IRSL and BLSL at different temperatures is further studied by investigating the relationship between the emitted light counts from the IRSL and the corresponding lost counts obtained from the pIR(T_1)-BLSL(T_2) experiments (T_1= 60, 100, 150, 200 °C; T_2= 60, 200 °C). This is similar to the method applied to study the relation between IRSL and thermoluminescence (TL) by Duller (1995). In Fig. 3, we plot the emitted counts from the IRSL, against the corresponding lost counts of the pIR-BLSL as a result of IR bleaching. It is observed that, if the stimulation temperature for IR and BL was identical in both cases (i.e. pIR(60)-BLSL(60) and pIR(200)-BLSL(200)), the emitted counts of the IRSL have a nearly 1:1 relationship with the corresponding lost counts in the pIR-BLSL. However, in the case of $T_1>T_2$, the emitted counts of the IRSL are larger than the corresponding lost counts in pIR-BLSL, indicating that the relationship between BLSL and IRSL is dependent on the stimulation temperature. It is to be noted that such a relationship between IRSL and BLSL is not influenced by the interference of isothermal TL, because the preheat at 280 °C for 10 s is sufficient to remove any isothermal TL at 200 °C. One straightforward explanation for the temperature dependency of the relationship is that at least two components are involved in the IRSL at the relatively high temperature (such as the IRSL at 200 °C). One component is responsive to the BL at 60 °C. The other is hard to reach by BL at 60 °C, but can be accessed at higher temperatures. The results further support fact that the IRSL signals at relatively high temperatures are relatively harder to bleach than the IRSL at 60 °C (e.g. Chen et al., 2013).

3.1.2 pBL-IRSL experiments

The effects of BL bleaching at 60 °C and 200 °C on the IRSL signals at different temperatures (60, 100, 150 and 200 °C) are investigated using pBL-IRSL experiments (see the procedures listed in Table 1). The experiments conducted are pBL(60)-IRSL(60), pBL(60)-IRSL(100), pBL(60)-IRSL(150), pBL(60)-IRSL(200) and pBL(200)-IRSL(200), respectively. Four aliquots of K-feldspar grains of HSDK-11 were firstly heated to 500 °C to remove any residual signals and then given the same irradiation dose of 30.4 Gy. These aliquots were then held at 280 °C for 10 s. They were subsequently bleached with BL at 60, 200 °C for different periods from 0 to 320 s before IRSL measurements. After that, the IRSL sensitivity was monitored and measured following a test dose of 15.2 Gy and preheat at 280 °C for 10 s.

The remnant IRSL at different temperatures (50, 100, 150 200 °C) as a result of BL bleaching at 60, 200 °C for different periods of time are shown in Fig. 4. It is demonstrated that the IRSL at 60 °C can be bleached to a negligible level (~0.2 %) by BL stimulation at 60 °C for 320 s, while 3.5 % of the initial IRSL at 200 °C still remains after BL bleaching at 60 °C for 320 s. These results indicate that, compared with the IRSL at 60 °C, the IRSL at 200 °C involves more traps that are harder to bleach by BL at 60 °C. However, the IRSL at 200 °C can be bleached to a negligible level (~0.2 %) by BL stimulation at 200 °C for 320 s. In addition, the decay rates in the pBL(200)-IRSL (200) and the pBL(60)-IRSL(60) are very similar and they are calculated at 0.23 ±0.02 s^{-1} and 0.21 ±0.01 s^{-1}, respectively. These results further suggest that the relationship between the IRSL and the BLSL is dependent on stimulation temperature.

Further investigation is made on the relationship between the emitted counts from the BLSL and the corresponding lost counts from pBL(T_1)-IRSL(T_2) (T_1= 60, 200 °C; T_2= 60, 100, 150, 200 °C) (Fig. 5). It is observed that the emitted counts from the BLSL measured both at 60 °C and at 200 °C are significantly larger than the corresponding lost counts from pBL(T_1)-IRSL(T_2). These results indicate that BL can access much more traps than IR stimulation. Only part of traps associated with the BLSL at 60 °C and at 200 °C is accessible by IR stimulation, which is similar to the results of IRSL observed at 60 °C (Gong et al, 2012). It is also demonstrated that relationship between emitted BLSL counts and lost counts of pBL-IRSL changes as the stimulation temperature changes.

To further demonstrate the relationship between different OSL components of the BLSL signal at 60 °C and the IRSL signals at relatively high temperatures, the emitted light counts from different OSL components of the BLSL signal at 60 °C are compared with the corresponding lost counts from the pBL(60)-IRSL(200) and pBL(60)-IRSL(60) as a result of BL bleaching at 60 °C for different periods. We plot the emitted counts from the various OSL components of the BLSL at 60 °C, against the lost counts of IRSL at 60 °C and IRSL at 200 °C as a result of BL bleaching in Fig. 6. It is observed that the lost counts in pBL(60)-IRSL(200) are larger than the sum of the emitted light counts of the fast and medium components of BLSL at 60 °C, while the lost counts in pBL(60)-IRSL(60) have a nearly 1:1 relationship with the sum of the emitted light counts of the fast and medium components of BLSL at 60 °C. These results indicate that the IRSL signals at 200 °C are involved with not only the fast and medium components of BLSL at 60 °C, but also some other OSL components (e.g. slower components of BLSL at 60 °C). In contrast, there is a close relationship between IRSL at 60 °C and the fast and medium components of BLSL at 60 °C (Gong et al., 2012). The results are consistent with the observations in previous section 3.1.1.

In summary, the results from the pIR-BLSL and pBL-IRSL bleaching experiments suggest that the relationship between IRSL and BLSL is dependent on stimulation temperature. At least two components of traps are involved in the IRSL measured at elevated temperatures (e.g., 200 °C). One component can be easily bleached by BL at 60 °C, and the other of the IRSL is relatively harder to access by BL at 60 °C. The results show that the IRSL signals at relatively high temperatures are harder to be bleached than the IRSL at room temperature.

3.2 Luminescence properties of IRSL at relatively high temperature

The luminescence characteristics of the IRSL at 200 °C, the pIR(60)-IRSL(200) and the pBL(60)-IRSL(200), including thermal stability, dose response and laboratory fading rate, were further investigated. In both the pIR(60)-IRSL(200) and the pBL(60)-IRSL(200) experiments, the IR and BL bleaching time was both fixed at 200 s.

3.2.1 Thermal stability study

The thermal stability studies are carried out using the pulse annealing test (Table 2) (Li et al., 1997; Li and Tso, 1997). The tests were conducted for the IRSL at 60 °C, the IRSL at 200 °C, the pIR(60)-IRSL(200) and the pBL(60)-IRSL(200), respectively. An aliquot of K-feldspar of SY was firstly heated to 500 °C and then given an irradiation dose of 30.4 Gy. After that, it was preheated at 280 °C for 10 s and then heated to a temperature at T °C before the remaining IRSL was measured at 60 °C for 160 s. The sensitivity change was monitored by measuring the IRSL signal at 60 °C from a test dose of 30.4 Gy. The same preheat condition (280 °C for 10 s) was applied for the test dose IRSL measurement. This cycle was repeated by increasing the annealing temperature (T) from 160 °C to 500 °C in steps of 20 °C. The similar pulse annealing test procedures were also conducted for the IRSL at 200 °C, the pIR(60)-IRSL(200) and the pBL(60)-IRSL(200) (Table 2). The heating rate for all these pulse annealing experiments was 3 $°C·s^{-1}$.

The typical decay curve of the pBL(60)-IRSL(200) signal is shown in Fig. 7. The results of the pulse annealing test of the IRSL at 60 °C, the IRSL at 200 °C, the pIR(60)-IRSL(200) and the pBL(60)-IRSL(200) are shown in Fig. 8. It is observed that the thermal stability of the IRSL at 200 °C is relatively more stable than that of the IRSL at 60 °C. Li and Li (2011b; 2013) also observed the different thermal stabilities among the IRSL at different stimulation temperatures. In addition, it is found that both pIR(60)-IRSL(200) and pBL(60)-IRSL(200) is more thermally stable than IRSL at 200 °C. The results suggest that at least two components are involved in the IRSL at 200 °C and the components have significantly different thermal stability. Both IR at 60 °C and BL at 60 °C can remove the thermally relatively unstable component of IRSL 200 °C. It is interesting to be noted that the pBL(60)-IRSL(200) is significantly more thermally stable than pIR(60)-IRSL(200), indicating that the BL at 60 °C is more efficient than IR at 60 °C to reduce thermally unstable component in the IRSL at 200 °C.

3.2.2 Dose response curves

Different shapes of dose response curve (DRC) may provide an indication of different origins of different luminescence signals (Gong et al., 2012). Here we compare the DRC of the IRSL at 200 °C from K-feldspar with that of the pBL(60)-IRSL(200). Regenerative doses ranging from 0 to 1950 Gy were employed in a single aliquot regeneration (SAR) protocol for the IRSL at 200 °C. A test dose of 52 Gy was applied and the test dose signal (T_x) was measured to monitor and correct for sensitivity change. A recycle dose at 26 Gy was used and the recycling ratios all fall within the range of 1.0 ± 0.05 for the sample. The preheat temperature (held at 280 °C for 10 s) was the same for regeneration and test dose measurements. A cut-heat to 500 °C was used between each of the SAR cycles to clean the residual signals from the previous cycle. The IRSL signals L_x and T_x were calculated from the integrated photon counts in the first 1 s of stimulation, with subtraction of a background signal derived from the last 10 s of the 160 s stimulation. For construction the DRC of the pBL(60)-IRSL(200), a similar SAR procedure was applied, except that a BL bleaching at 60 °C for 200 s was added before each IRSL measurement for both the regenerative and test dose measurements. The dose response curves for the two signals are shown in Fig. 9. It is found that the pBL(60)-IRSL(200) signal have a different dose saturation level with the IRSL at 200 °C.

If the two dose response curves are fitted with double saturation exponential function (equation 1),

$$I = I_0 + I_a(1 - \exp(-D / D_{0,a}) + I_b(1 - \exp(-D / D_{0,b}) \qquad (1)$$

The dose saturation level of two D_0 ($D_{0,a}$ and $D_{0,b}$) parameters are 42.9±5.8 Gy and 289.7±22.4 Gy for the pBL(60)-IRSL(200) signal, while the values of two D_0 ($D_{0,a}$ and $D_{0,b}$) parameters of the IRSL at 200 °C are significantly higher at 214.6±9.9 Gy and 806.1 ± 69.6 Gy, respectively. The results indicate that at least two components are involved in the IRSL at elevated temperature. One group is easy to bleach by BL at 60 °C and they have a higher dose saturation level, while the other group is hard to bleach by BL at 60 °C and they have a lower dose saturation level.

3.2.3 Laboratory fading test

Anomalous fading was observed for both IRSL and BLSL signals in previous studies (e.g. Thomsen et al., 2008). Here we studied the laboratory fading rates for the IRSL at 200 °C, the pIR(60)-IRSL(200) and the pBL(60)-IRSL(200) signals. In measurement of the IRSL at 200 °C, six aliquots of SY were heated to 500 °C to remove any residual signals (similar to a hot-bleach between SAR cycles). Then these aliquots were given 50.8 Gy and immediately preheated at 280 °C for 10 s. The sensitivity corrected signals were then measured after delays of different periods. For the test dose, 12.7 Gy was given and the same preheat condition was applied. The IRSL signals $L_{(x)}$ and $T_{(x)}$ were calculated from the integrated photon counts in the first 1 s of stimulation, with subtraction of a background signal derived from the last 10 s of the 160 s stimulation. The first measurement of the IRSL at 200 °C signal took place at a time t_c= 562 s after the mid-point of the irradiation time. A similar measurement procedure was adopted for measuring the fading rate for the pIR(60)-IRSL(200) and pBL(60)-IRSL(200) signals. For the pIR(60)-IRSL(200) signal, an IR bleaching at 60 °C for 200 s was added before the IRSL measurement at 200 °C for both the regenerative and test dose measurements. The first measurement of the pIR(60)-IRSL(200) signal took place at a time t_c= 669 s after the mid-point of the irradiation time. For the pBL(60)-IRSL(200) signal, a BL bleaching at 60 °C for 200 s was added before the IRSL measurement at 200 °C for both the regenerative and test dose measurements. The first measurement of the pBL(60)-IRSL(200) signal took place at a time t_c= 669 s after the mid-point of the irradiation time. The decay of the IRSL at 200 °C, the pIR(60)-IRSL(200) and the pBL(60)-IRSL(200) signals after normalization as a function of storage time is shown in Fig 10. The corresponding anomalous fading rates (g-value) are calculated based on the data sets and are also shown in Fig. 10. It is observed that the IRSL at 200 °C, the pIR(60)-IRSL(200) and the pBL(60)-IRSL(200) have significantly different laboratory fading rates. The g value for the IRSL at 200 °C was detected at 4.0±0.3 %/decade, the g value of the pIR(60)-IRSL(200) was at 1.6±0.4 %/decade and the pBL(60)-IRSL(200) was 0.4±0.4 %/decade. This result indicates that there are at least two components for the IRSL at 200 °C. One component is easy to bleach by IR at 60 °C and BL at 60 °C and it has higher laboratory fading rate, while the other is hard to bleach by IR at 60 °C and BL at 60 °C and it has a significantly lower fading rate.

4. Discussion

The sources and process of the traps associated with IRSL from feldspar are important for developing reliable dating methods. Different models have been proposed to explain the various luminescence behaviors of feldspars. A single trap model has been proposed recently to explain the luminescence characteristics for feldspar (e.g., Jain and Ankjærgaard, 2011; Anderson et al., 2012), while a multi-trap model is suggested alternatively by others (e.g., Duller and Bøtter-Jensen, 1993; Li and Li, 2011; Thomsen et al., 2011; Li et al., 2014). These studies were based on their own experimental designs with limited experimental conditions and the explanations are based on different assumptions, so a unique interpretation cannot be reached. It is hoped that the study of the relationship between BLSL and IRSL could be helpful for understanding the source and process of IRSL, because, unlike IRSL process, BLSL is expected to be a simpler and delocalized process due to the higher photon energy of BL (~2.64 eV) compared to the main IRSL trap depth (~2.5 eV) (e.g. Baril and Huntley, 2003; Kars et al., 2013). Based on our results, we are in favor of the multiple-trap model to explain the experimental data obtained in this study, which cannot be well explained using a simple single-trap model. The pieces of evidence are given as follows:

(1) If we assume that IRSL at 200 °C and 60 °C originate the same traps and then both signals should be depleted by BL at a similar rate, because BL have energy high enough to evict the trapped electron to the conduction band and then the electron can randomly recombine with both close and distant holes. In Fig. 4, it is clearly shown that, compared with the IRSL at 60 °C, the IRSL at 200 °C is bleached at the significantly slower rate by BL at 60 °C, suggesting that IRSL signals at 200 °C are involved with traps which are very hard to bleach by BL at 60 °C. This could be due to either that the hard-to-bleach component has a deeper trap depth (>2.5 eV) or that the component has a different photoionization cross-section, which both indicate a different trap from the easy to bleach component.

(2) During the pIR(60)-BLSL(60) experiments, the emitted counts of the IRSL have a nearly 1:1 relationship with the corresponding lost counts in the pIR-BLSL. However, this is not the case for the pIR(200)-BLSL(60) (Fig. 3). This indicates that IRSL at elevated temperature can access more traps that are more difficult to bleach by BL at 60 °C.

(3) The pBL(60)-IRSL(200) and IRSL signals at 200 °C have very different luminescence properties, such as thermal stability, dose response and fading rate. Since BL have energy high enough to evict the trapped electron to the conduction band, the electron will randomly recombine with close or distant holes after excitation. Hence, BL will cause not only recombination of spatially close electron-hole pairs, but also recombination of distant electron-hole pairs. As a result, BL bleaching should not change the relative proportions between close and distant electron-hole pairs. Correspondingly, it is expected that the pBL-IRSL should have a similar thermal stability as IRSL, and the pIR-IRSL should have a higher thermal stability than pBL-IRSL. Our results, however, showed that the pBL(60)-IRSL(200) is significantly more thermally stable than both the IRSL at 200 °C and pIR(60)-IRSL(200) (Fig. 8), which cannot be explained by the single-trap model. Similarly, a similar fading rate should be expected for the IRSL(200) and pBL(60)-IRSL(200) signals based on a single-trap model. For our samples, the g values for the IRSL at 200 °C are greatly reduced after the BL bleaching at 60 °C for 200 s (Fig. 10). It is interesting to be

noted that the laboratory fading rate of pBL(60)-IRSL(200) is significantly lower than that of pIR(60)-IRSL(200), suggesting that the BL at 60 °C is more efficiently than the IR at 60 °C to remove spatially close electron-hole pairs (easy-to-fade), which cannot be explained by a single trap model.

Based on the above arguments, we think that a single trap model is not sufficient to explain all the luminescence phenomena in feldspar. In the future, it is maybe helpful to use time-resolved optically stimulated luminescence (TR-OSL) technique to further study the luminescence behaviors of K-feldspar (e.g. Chithambo and Galloway, 2001).

Another outcome of our study is that we first demonstrate that the pBL(60)-IRSL(200) has a high thermal stability and a negligible fading rate, which opens the potential of using this signal in sediments dating without the corrections for anomalous fading. A potential advantage of using pBL(60)-IRSL(200) is that blue bleaching at 60 °C can eliminate the contribution of quartz grains to IRSL at elevated temperatures (Fan et al., 2009). Quartz grains can coexist with K-feldspar after heavy liquid separation. The IRSL of quartz at elevated temperatures can be effectively bleached by blue light at low temperatures, but not by infrared. Further tests on the applicability in dating are required to confirm the suitability of using the pBL-IRSL at relatively high temperatures.

5. Conclusions

From the pIR-BLSL and pBL-IRSL bleaching experiments, it is concluded that the relationship between IRSL and BLSL is dependent on the stimulation temperature. If stimulation temperatures for the IRSL increase from 60 to 200 °C, at least two components are associated with the IRSL at 200 °C. One component is easy to bleach by BL at 60 °C, and the other relative hard to bleach by BL at 60 °C. The two components of the IRSL at 200 °C have significantly different luminescence properties, in terms of thermal stability, dose saturation level and laboratory fading rates.

Acknowledgments

This study was financially supported by the grants to Sheng-Hua Li from the Research Grant Council of the Hong Kong Special Administrative Region, China (Project nos. 7028/08P and 7033/12P). The authors are grateful to the two anonymous reviewers for providing valuable comments and suggestions on the manuscript.

Reference

Adamiec, G., 2005. OSL decay curves—relationship between single- and multiple-grain aliquots. Radiation Measurements 39, 63-75.

Aitken, M.J., 1998. An Introduction to Optical Dating. Oxford Unversity Press, Oxford.

Andersen, M.T., Jain, M., Tidemand-Lichtenberg, P., 2012. Red-IR stimulated luminescence in K-feldspar: Single or multiple trap origin? Journal of Applied Physics 112, 043507, DOI 10.1063/1.4745018.

Bøtter-Jensen, L., Andersen, C.E., Duller, G.A.T., Murray, A.S., 2003. Developments in radiation, stimulation and observation facilities in luminescence measurements. Radiation Measurements 37, 535-541.

Baril, M. R., and Huntley, D. J., 2003, Optical excitation spectra of trapped electrons in irradiated feldspars: Journal of Physics-Condensed Matter, v. 15, no. 46, p. 8011-8027.

Buylaert, J.P., Jain, M., Murray, A.S., Thomsen, K.J., Thiel, C., and Sohbati, R., 2012, A robust feldspar luminescence dating method for Middle and Late Pleistocene sediments. Boreas 41, 435-451.

Buylaert, J.P., Murray, A.S., Thomsen, K.J., Jain, M., 2009. Testing the potential of an elevated temperature IRSL signal from K-feldspar. Radiation Measurements 44, 560-565.

Buylaert, J.P., Thiel, C., Murray, A., Vandenberghe, D.G., Yi, S., Lu, H., 2011. IRSL and post-IR IRSL residual doses recorded in modern dust samples from the Chinese Loess Plateau. Geochronometria 38, 432-440.

Chen, Y., Li, S.-H., Li, B., 2013. Residual doses and sensitivity change of post IR IRSL signals from potassium feldspar under different bleaching conditions. Geochronometria 40, 229-238.

Chithambo, M.L., Galloway, R.B., 2001. On the slow component of luminescence stimulated from quartz by pulsed blue light-emitting diodes. Nuclear Instruments and Methods in Physics Research Section B: Beam Interactions with Materials and Atoms 183, 358-368.

Duller, G.A.T., 1995. Infrared bleaching of the thermoluminescence of four feldspars. Journal of Physics D: Applied Physics 28, 1244.

Duller, G.A.T., Bøtter-Jensen, L., 1993. Luminescence from Potassium Feldspars Stimulated by Infrared and Green Light. Radiation Protection Dosimetry 47, 683-688.

Fan, A.C., Li, S.-H., Li, B., 2009. Characteristics of quartz infrared stimulated luminescence (IRSL) at elevated temperatures. Radiation Measurements 44, 434-438.

Galloway, R.B., 1994. Comparison of the green- and infrared-stimulated luminescence of feldspar. Radiation Measurements 23, 617-620.

Gong, Z., Li, B., Li, S.-H., 2012. Study of the relationship between infrared stimulated luminescence and blue light stimulated luminescence for potassium-feldspar from sediments. Radiation Measurements 47, 841-845.

Gong, Z., Li, S.-H., Sun, J., Xue, L., 2013. Environmental changes in Hunshandake (Otindag) sandy land revealed by optical dating and multi-proxy study of dune sands. Journal of Asian Earth Sciences 76, 30-36.

Hütt, G., Jaek, I., Tchonka, J., 1988. Optical Dating: K-Feldspars Optical Response Stimulation Spectra. Quaternary Science Reviews 7, 381-385.

Huntley, D.J., Lamothe, M., 2001. Ubiquity of anomalous fading in K-feldspars and the measurement and correction for it in optical dating. Canadian Journal of Earth Sciences 38, 1093-1106.

Jain, M., Ankjærgaard, C., 2011. Towards a non-fading signal in feldspar: Insight into charge transport and tunnelling from time-resolved optically stimulated luminescence. Radiation Measurements 46, 292-309.

Jain, M., Singhvi, A.K., 2001. Limits to depletion of blue-green light stimulated luminescence in feldspars: implications for quartz dating. Radiation Measurements 33, 883-892.

Kars, R.H., et al., 2013. On the trap depth of the IR-sensitive trap in Na- and K-feldspar. Radiation Measurements 59, 103-113.

Li, B., 2010. The relationship between thermal activation energy, infrared stimulated luminescence and anomalous fading of K-feldspars. Radiation Measurements 45, 757-763.

Li, B., Jacobs, Z., Roberts, R.G., Li, S.-H., 2013. Extending the age limit of luminescence dating using the dose-dependent sensitivity of MET-pIRIR signals from K-feldspar. Quaternary Geochronology 17, 55-67.

Li, B., Jacobs, Z., Roberts, R., Li, S.-H., 2014b, Review and assessment of the potential of post-IR IRSL dating methods to circumvent the problem of anomalous fading in feldspar luminescence. Geochronometria, 41, 178-201.

Li, B., Li, S.-H., 2008. Investigations of the dose-dependent anomalous fading rate of feldspar from sediments. Journal of Physics D-Applied Physics 41, 225502.

Li, B., Li, S.-H., 2011a. Luminescence dating of K-feldspar from sediments: A protocol without anomalous fading correction. Quaternary Geochronology 6, 468-479.

Li, B., Li, S.-H., 2011b. Thermal stability of infrared stimulated luminescence of sedimentary K- feldspar. Radiation Measurements 46, 29-36.

Li, B., Li, S.-H., 2012. Luminescence dating of Chinese loess beyond 130 ka using the non-fading signal from K-feldspar. Quaternary Geochronology 10, 24-31.

Li, B., Li, S.-H., 2013. The effect of band-tail states on the thermal stability of the infrared stimulated luminescence from K-feldspar. Journal of Luminescence 136, 5-10.

Li, B., Li, S.-H., Wintle, A.G., Zhao, H., 2007a. Isochron measurements of naturally irradiated K- feldspar grains. Radiation Measurements 42, 1315-1327.

Li, B., Roberts, R.G., Jacobs, Z., Li, S.-H., 2014a. A single-aliquot luminescence dating procedure for K-feldspar based on the dose-dependent MET-pIRIR signal sensitivity. Quaternary Geochronology 20, 51-64.

Li, S.-H., Chen, Y.Y., Li, B., Sun, J.M., Yang, L.R., 2007b. OSL dating of sediments from desert in northern China. Quaternary Geochronology 2, 23-28.

Li, S.-H., Sun, J.M., Zhao, H., 2002. Optical dating of dune sands in the northeastern deserts of China. Palaeogeography Palaeoclimatology Palaeoecology 181, 419-429.

Li, S.-H., Tso, M.Y.W., 1997. Lifetime determination of OSL signals from potassium feldspar. Radiation Measurements 27, 119-121.

Li, S.-H., Tso, M.Y.W., Wong, N.W.L., 1997. Parameters of OSL traps determined with various linear heating rates. Radiation Measurements 27, 43-47.

Lowick, S.E., Trauerstein, M., and Preusser, F., 2012, Testing the application of post IR-IRSL dating to fine grain waterlain sediments. Quaternary Geochronology 8, 33-40.

Murray, A.S., Thomsen, K.J., Masuda, N., Buylaert, J.P., and Jain, M., 2012, Identifying well-bleached quartz using the different bleaching rates of quartz and feldspar luminescence signals: Radiation Measurements 47, 688-695.

Spooner, N.A., 1994. The anomalous fading of infrared-stimulated luminescence from feldspars. Radiation Measurements 23, 625-632.

Thiel, C., Buylaert, J.-P., Murray, A., Terhorst, B., Hofer, I., Tsukamoto, S., Frechen, M., 2011. Luminescence dating of the Stratzing loess profile (Austria) - Testing the potential of an elevated temperature post-IR IRSL protocol. Quaternary International 234, 23-31.

Thomsen, K.J., Murray, A.S., Jain, M., 2011. Stability of IRSL signals from sedimentary K-feldspar samples. Geochronometria 38, 1-13.

Thomsen, K.J., Murray, A.S., Jain, M., Bøtter-Jensen, L., 2008. Laboratory fading rates of various luminescence signals from feldspar-rich sediment extracts. Radiation Measurements 43, 1474-1486.

Figure captions

Figure 1: Remnant BLSL measured at 60 °C and 200 °C after IR bleaching at different temperature for different times. The temperatures for IR bleaching were set at 60, 100, 150 and 200 °C, respectively.

Figure 2: (a) four representative pIR-BLSL signals, which are then deconvoluted into three components. For each of the fitting, the F-statistics are provided and they are all significantly larger than $F_{0.01}$ (e.g. Adamiec, 2005). The corresponding residuals are shown at the right. (b) The residual fast, medium and slow components of BLSL at 60 °C after IR bleaching for different time from 0 s to 5000 s. To better demonstrate the data, the residual fast and medium components of BLSL at 60 °C after IR bleaching for different time from 0 s to 320 s were further shown in the insets, while the y-axis in the insets is on the logarithmic scale. The data were from sample HSDK-11 and the fast, medium and slow components of BLSL at 60 °C were fitted with the decay rates of 0.375 ± 0.004 s^{-1}, 0.077 ± 0.002 s^{-1} and 0.0072 ± 0.0002 s^{-1}, respectively, the same as Gong et al. (2012).

Figure 3: The relationship between emitted counts of the IRSL and the corresponding lost counts of pIR(T_1)-BLSL(T_2) as a result of IR bleaching for different time. T_1= 60, 100, 150, 200 °C, T_2= 60, 200 °C respectively.

Figure 4: Remnant IRSL after blue light bleaching at 60 °C and 200 °C for different times. The temperatures for IR stimulations were set at 60, 100, 150 and 200 °C, respectively.

Figure 5: The relationship between emitted counts of the BLSL and the corresponding lost counts of pBL(T_1)-IRSL(T_2) as a result of blue light bleaching for different time. T_1= 60, 200 °C, T_2= 60, 100, 150, 200 °C, respectively.

Figure 6: The relationship between emitted counts of OSL components of BLSL at 60 °C and the lost counts of pBL(60)-IRSL(200) and pBL(60)-IRSL(60) as a result of blue light bleaching at 60 °C for different times. F+M: The sum of fast and medium components of the BLSL at 60 °C; S: slow component of the BLSL at 60 °C. The data were from sample HSDK-11.

Figure 7: The typical decay curves of the pBL(60)-IRSL(200) from sample HSDK-11. All the signals were normalized using the initial intensity of the pBL(60)-IRSL(200).

Figure 8: Pulse annealing curves based on the IRSL signal at 60 °C, the IRSL signal at 200 °C, pIR(60)-IRSL(200) and the pBL(60)-IRSL(200) signal; In the pIR(60)-IRSL(200) and pBL(60)-IRSL(200) experiments, the previous IR stimulation and BL stimulation at 60 °C are both at 200 s. The heating rate was 3 $°C \cdot s^{-1}$.

Figure 9: Dose response curves of the IRSL signal at 200 °C and the pBL(60)-IRSL(200) signal. The two dose response curves could be fitted well by the double saturation exponential function (R^2>0.99; residuals are shown in the inset).

Figure 10: Anomalous fading tests for IRSL signal at 200 °C, the pIR(60)-IRSL(200) and the pBL(60)-IRSL(200) signal using six aliquots from sample SY as a function of delayed period (t).

Figure 1

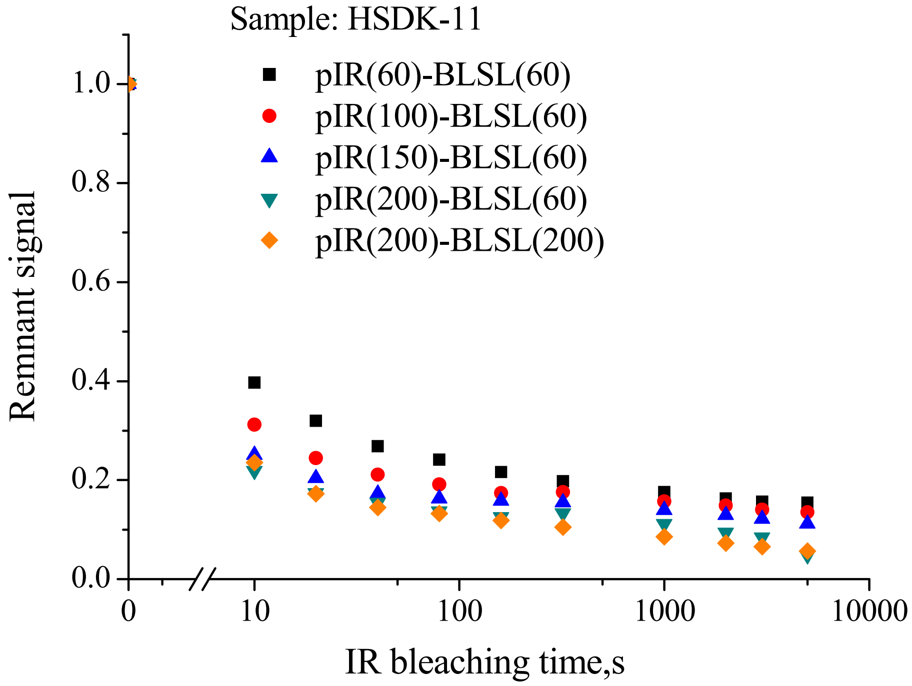
Sample: HSDK-11
pIR(60)-BLSL(60)
pIR(100)-BLSL(60)
pIR(150)-BLSL(60)
pIR(200)-BLSL(60)
pIR(200)-BLSL(200)
Remnant signal
1.0
0.8
0.6
0.4
0.2
0.0
0
10
100
1000
10000
IR bleaching time,s

Figure 2a

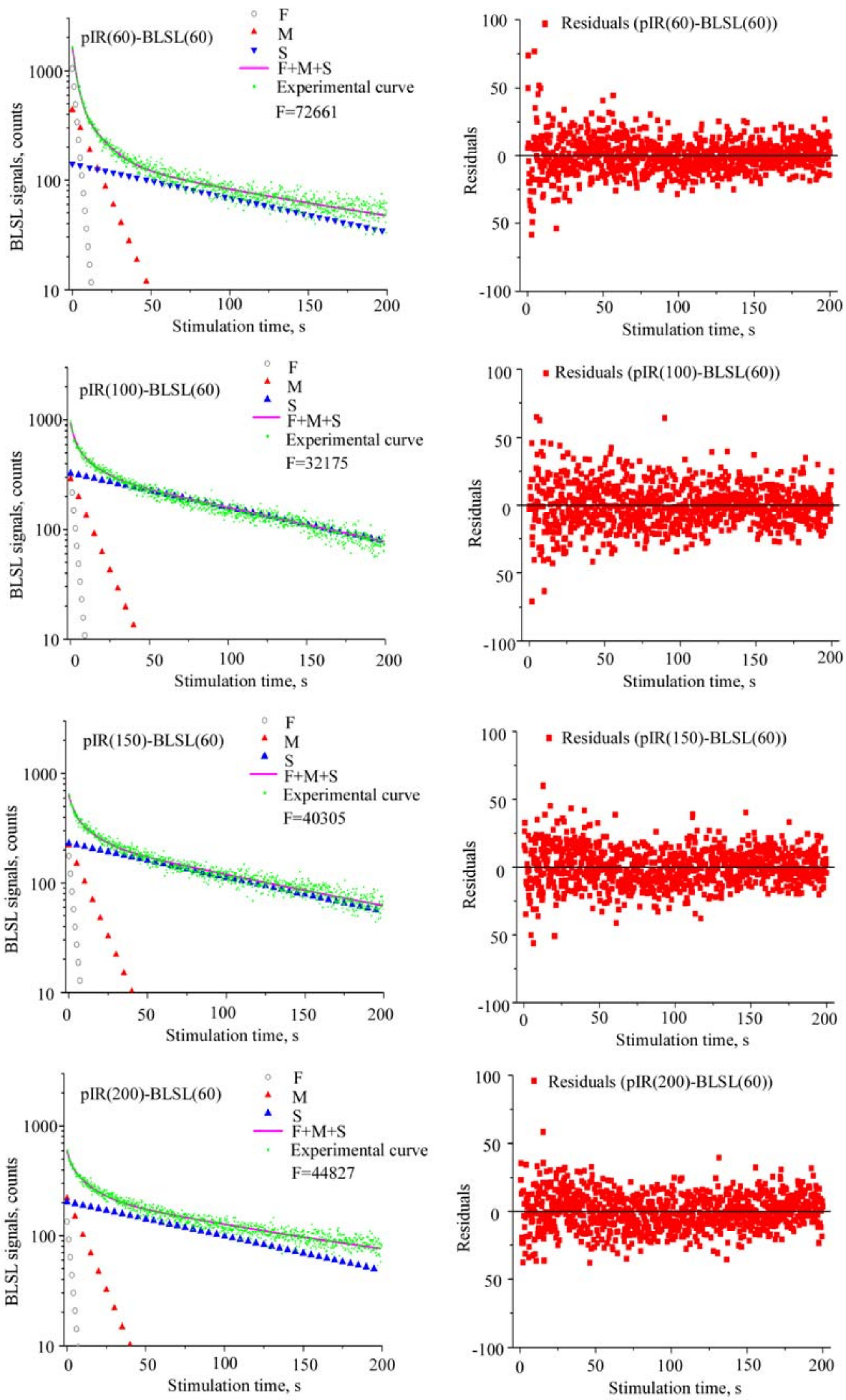
pIR(60)-BLSL(60)
F
M
S
F+M+S
Experimental curve
F=72661
BLSL signals, counts
Stimulation time, s
Residuals (pIR(60)-BLSL(60))
Residuals
Stimulation time, s
pIR(100)-BLSL(60)
F
M
S
F+M+S
Experimental curve
F=32175
BLSL signals, counts
Stimulation time, s
Residuals (pIR(100)-BLSL(60))
Residuals
Stimulation time, s
pIR(150)-BLSL(60)
F
M
S
F+M+S
Experimental curve
F=40305
BLSL signals, counts
Stimulation time, s
Residuals (pIR(150)-BLSL(60))
Residuals
Stimulation time, s
pIR(200)-BLSL(60)
F
M
S
F+M+S
Experimental curve
F=44827
BLSL signals, counts
Stimulation time, s
Residuals (pIR(200)-BLSL(60))
Residuals
Stimulation time, s

Figure 2b

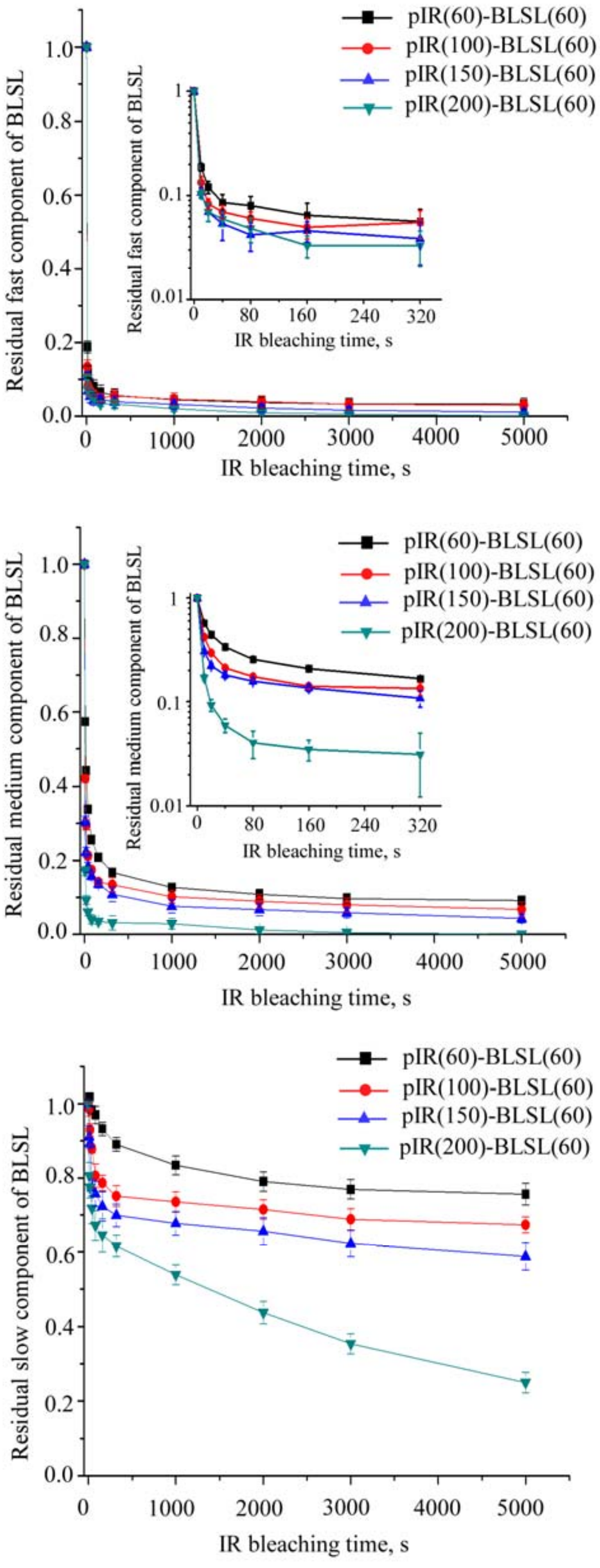

pIR(60)-BLSL(60)
pIR(100)-BLSL(60)
pIR(150)-BLSL(60)
pIR(200)-BLSL(60)
Residual fast component of BLSL
1.0
0.8
0.6
0.4
0.2
0.0
0
1000
2000
3000
4000
5000
IR bleaching time, s
Residual fast component of BLSL
1
0.1
0.01
0
80
160
240
320
IR bleaching time, s
pIR(60)-BLSL(60)
pIR(100)-BLSL(60)
pIR(150)-BLSL(60)
pIR(200)-BLSL(60)
Residual medium component of BLSL
1.0
0.8
0.6
0.4
0.2
0.0
0
1000
2000
3000
4000
5000
IR bleaching time, s
Residual medium component of BLSL
1
0.1
0.01
0
80
160
240
320
IR bleaching time, s
pIR(60)-BLSL(60)
pIR(100)-BLSL(60)
pIR(150)-BLSL(60)
pIR(200)-BLSL(60)
Residual slow component of BLSL
1.0
0.8
0.6
0.4
0.2
0.0
0
1000
2000
3000
4000
5000
IR bleaching time, s

Figure 3

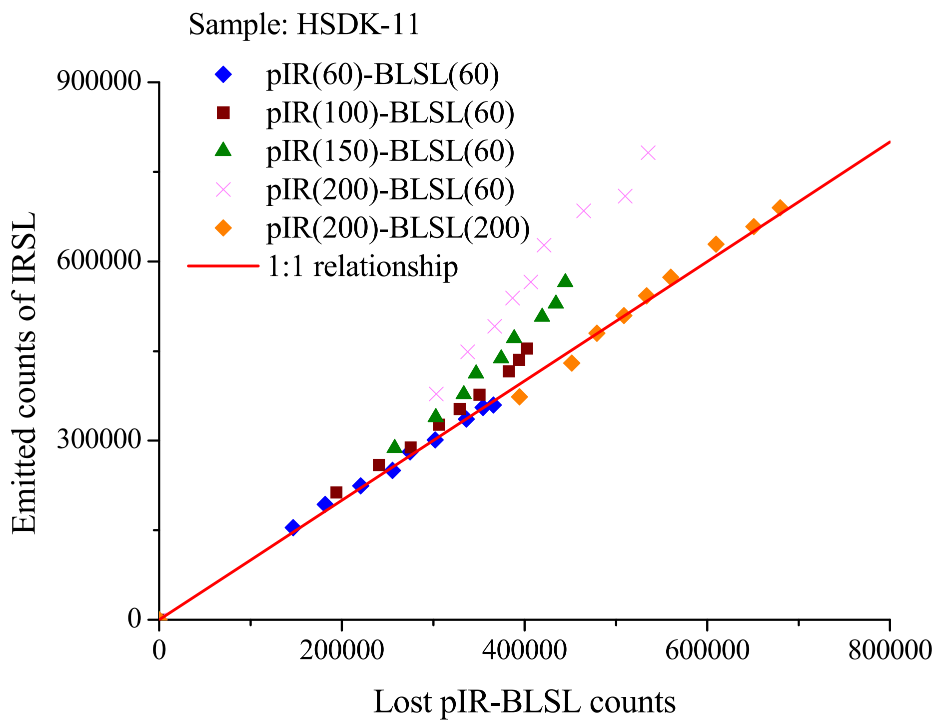

Sample: HSDK-11
pIR(60)-BLSL(60)
pIR(100)-BLSL(60)
pIR(150)-BLSL(60)
pIR(200)-BLSL(60)
pIR(200)-BLSL(200)
1:1 relationship
900000
600000
300000
0
0
200000
400000
600000
800000
Emitted counts of IRSL
Lost pIR-BLSL counts

Figure 4

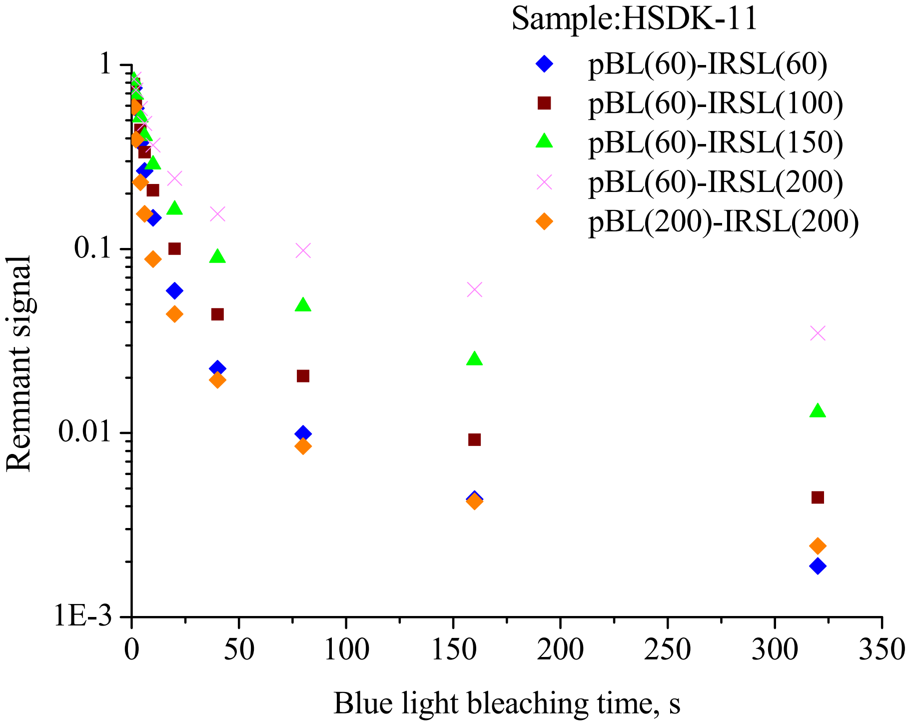

Sample:HSDK-11
pBL(60)-IRSL(60)
pBL(60)-IRSL(100)
pBL(60)-IRSL(150)
pBL(60)-IRSL(200)
pBL(200)-IRSL(200)
Remnant signal
1
0.1
0.01
1E-3
0
50
100
150
200
250
300
350
Blue light bleaching time, s

Figure 5

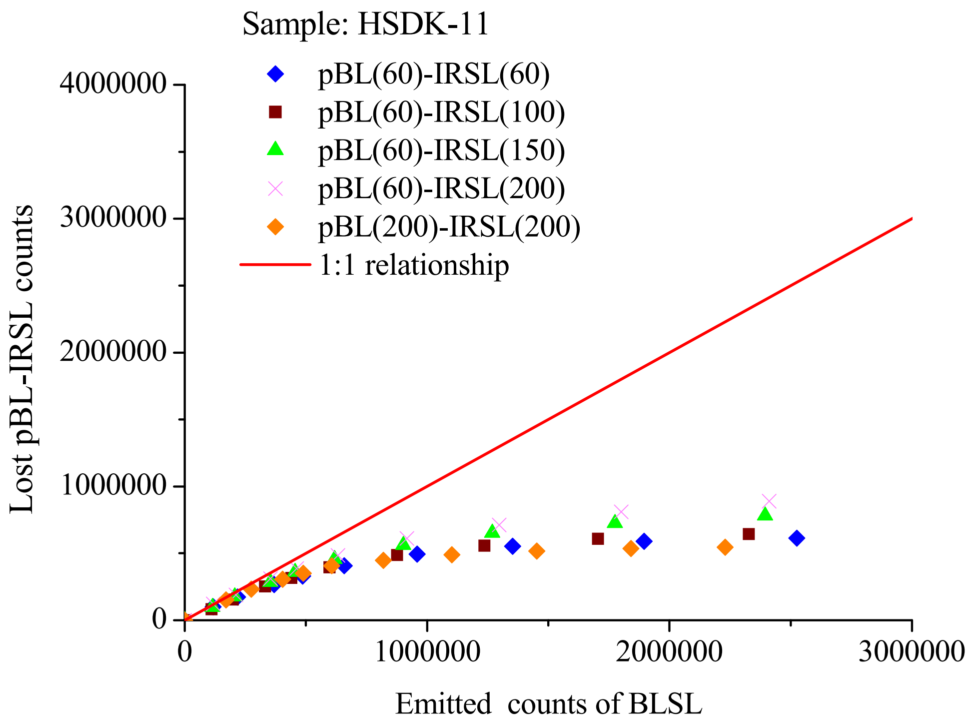

Sample: HSDK-11
pBL(60)-IRSL(60)
pBL(60)-IRSL(100)
pBL(60)-IRSL(150)
pBL(60)-IRSL(200)
pBL(200)-IRSL(200)
1:1 relationship
Lost pBL-IRSL counts
4000000
3000000
2000000
1000000
0
0
1000000
2000000
3000000
Emitted counts of BLSL

Figure 6

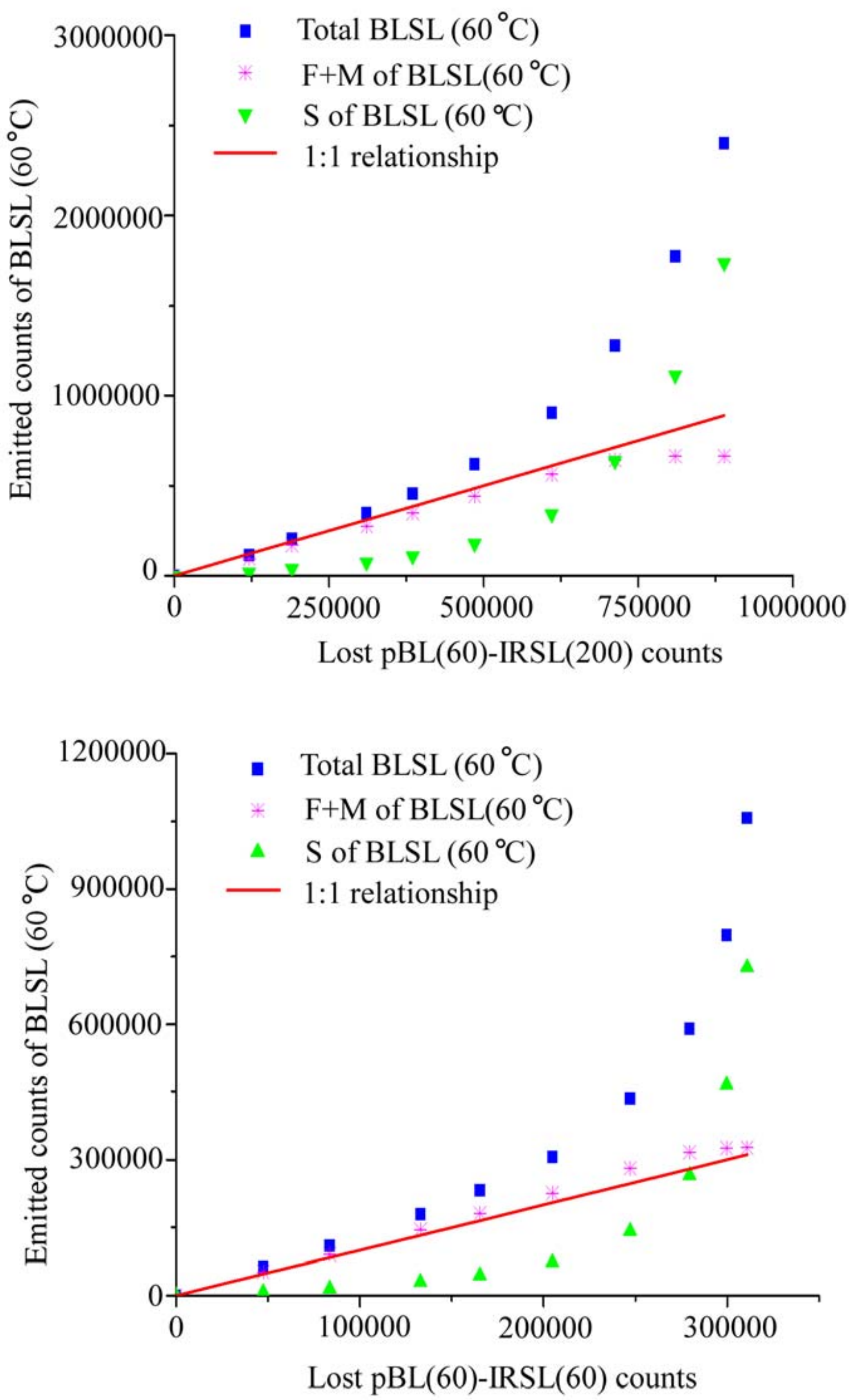

Total BLSL (60 °C)
F+M of BLSL(60 °C)
S of BLSL (60 °C)
1:1 relationship
3000000
2000000
1000000
0
Emitted counts of BLSL (60°C)
0
250000
500000
750000
1000000
Lost pBL(60)-IRSL(200) counts
Total BLSL (60 °C)
F+M of BLSL(60 °C)
S of BLSL (60 °C)
1:1 relationship
1200000
900000
600000
300000
0
Emitted counts of BLSL (60 °C)
0
100000
200000
300000
Lost pBL(60)-IRSL(60) counts

Figure 7

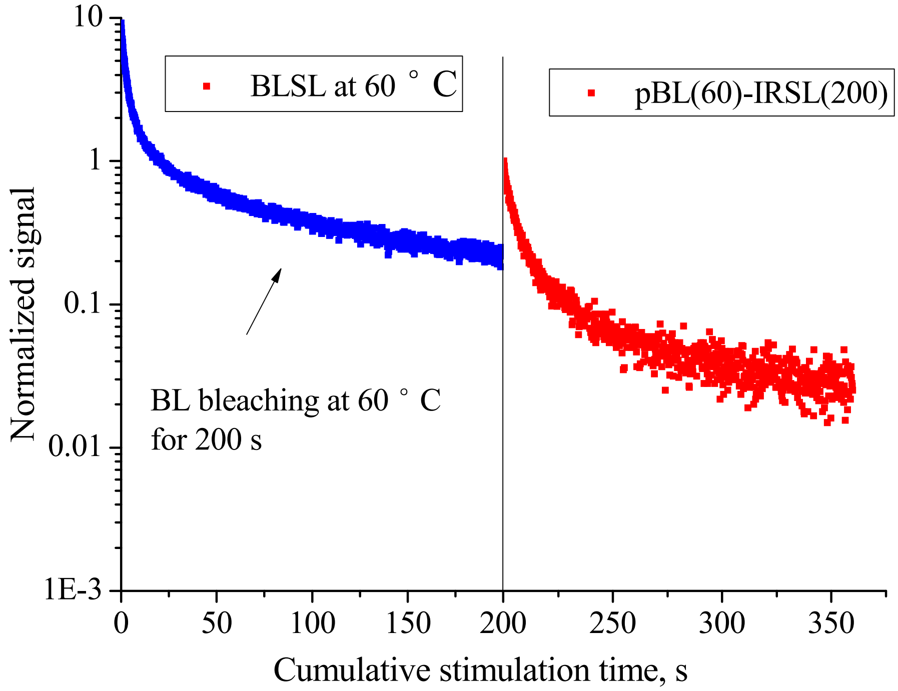
BLSL at 60 ° C
pBL(60)-IRSL(200)
BL bleaching at 60 ° C
for 200 s
Normalized signal
10
1
0.1
0.01
1E-3
0
50
100
150
200
250
300
350
Cumulative stimulation time, s

Figure 8

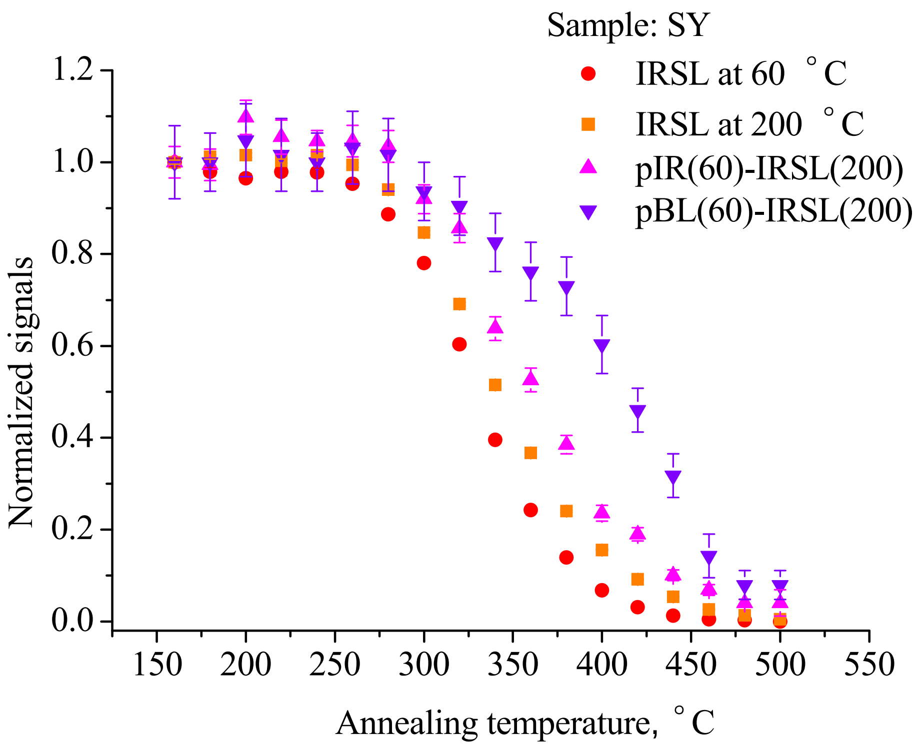

Sample: SY
IRSL at 60 °C
IRSL at 200 °C
pIR(60)-IRSL(200)
pBL(60)-IRSL(200)
Normalized signals
0.0
0.2
0.4
0.6
0.8
1.0
1.2
150
200
250
300
350
400
450
500
550
Annealing temperature, °C

Figure 9

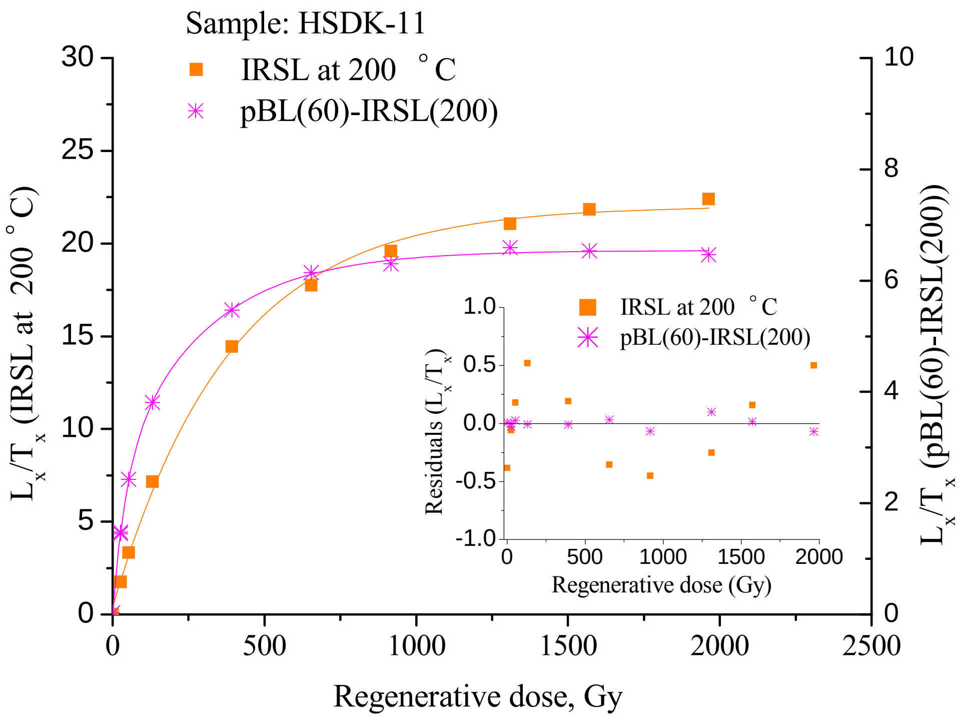
Sample: HSDK-11
IRSL at 200 °C
pBL(60)-IRSL(200)
L_x/T_x (IRSL at 200 °C)
L_x/T_x (pBL(60)-IRSL(200))
Regenerative dose, Gy
0
500
1000
1500
2000
2500
0
5
10
15
20
25
30
0
2
4
6
8
10
IRSL at 200 °C
pBL(60)-IRSL(200)
Residuals (L_x/T_x)
Regenerative dose (Gy)
1.0
0.5
0.0
-0.5
-1.0
0
500
1000
1500
2000

Figure 10

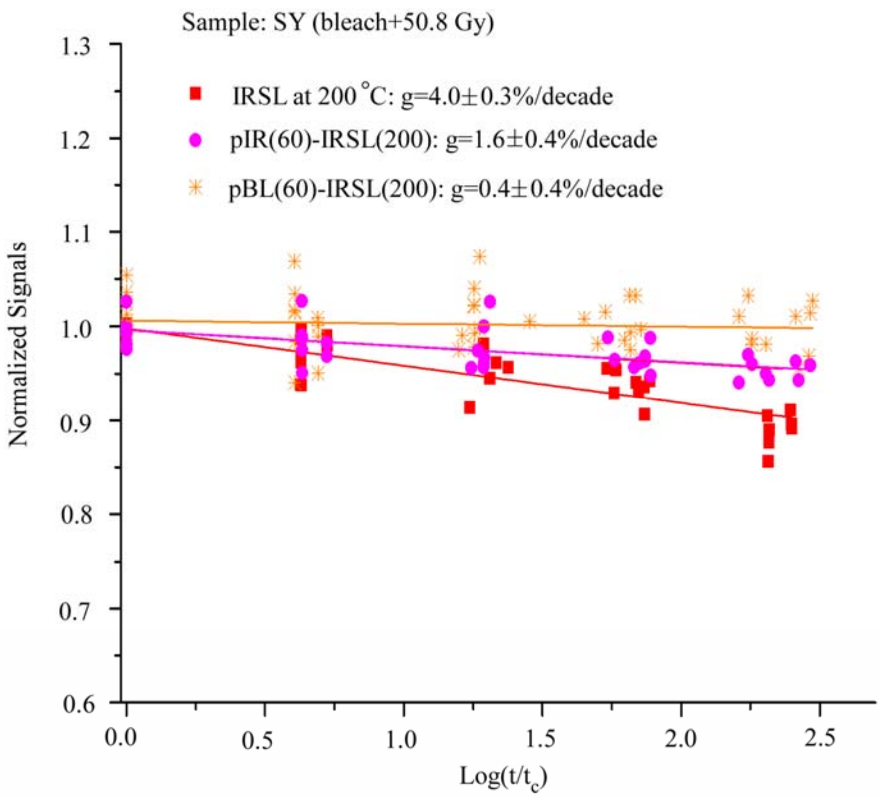
Sample: SY (bleach+50.8 Gy)
IRSL at 200 °C: g=4.0±0.3%/decade
pIR(60)-IRSL(200): g=1.6±0.4%/decade
pBL(60)-IRSL(200): g=0.4±0.4%/decade
Normalized Signals
1.3
1.2
1.1
1.0
0.9
0.8
0.7
0.6
0.0
0.5
1.0
1.5
2.0
2.5
Log(t/tc)

Table 1

Experimental procedures for the pIR(T_1)-BLSL(T_2) and pBL(T_2)-pIRSL(T_1) experiments. T_1 were set at 60,100, 150, 200 °C respectively, while T_2 were set at 60 and 200 °C.

	pIR(T_1)-BLSL(T_2)		pBL(T_2)-pIRSL(T_1)	
Step	Treatment	Observed	Treatment	Observed
(1)	Cut-heat to 500 °C		Cut-heat to 500 °C	
(2)	Regenerative dose (30.4 Gy)		Regenerative dose (30.4 Gy)	
(3)	Preheat to 280 °C for 10 s		Preheat to 280 °C for 10 s	
(4)	IR bleaching at T_1 for different time (0-5000 s)		BL bleaching at T_2 for different time (0-320 s)	
(5)	BLSL measurement at T_2 for 200 s	$L_{pIR\text{-}BLSL}$	IRSL measurement at T_1 for 160 s	$L_{pBL\text{-}IRSL}$
(6)	Test dose (15.2 Gy)		Test dose (15.2 Gy)	
(7)	Preheat to 280 °C for 10s		Preheat to 280 °C for 10s	
(8)	BLSL measurement at T_2 for 200 s	T_{BLSL}	IRSL measurement at T_1 for 160 s	T_{IRSL}
(9)	Return to step 1 and time for bleaching changes		Return to step 1 and time for bleaching changes	

Table 2

Pulse annealing procedures for the IRSL at 60 °C, the IRSL at 200 °C, the pIR(60)-IRSL(200) and the pBL(60)-IRSL(200). Note that the sequence of IRSL at 60 °C is steps 1, 2, 3, 4, 5a, 6, 7, 8a and 9, the sequence of IRSL at 200 °C is steps 1, 2, 3, 4, 5b, 6, 7, 8b and 9, the sequence of pIR(60)-IRSL(200) is steps 1, 2, 3, 3a, 4, 5b, 6, 7, 8b and 9 and the sequence of pBL(60)-IRSL(200) is steps 1, 2, 3, 3b, 4, 5b, 6, 7, 8b and 9.

Step	Treatment	Observed
(1)	Cut-heat to 500 °C	
(2)	Regenerative dose (30.4 Gy)	
(3)	Preheat to 280 °C for 10 s	
(3a)	IR bleaching at 60 °C for 200 s	
(3b)	BL bleaching at 60 °C for 200 s	
(4)	Cut-heat to T °C (160 °C -500 °C)	
(5a)	IRSL measurement at 60 °C for 160 s	$L_{(IRSL\ 60\ °C)}$
(5b)	IRSL measurement at 200 °C for 160 s	$L_{(IRSL\ 200\ °C)}$
(6)	Test dose (30.4 Gy)	
(7)	Preheat to 280 °C for 10 s	
(8a)	IRSL measurement at 60 °C for 160 s	$T_{(IRSL\ 60\ °C)}$
(8b)	IRSL measurement at 200 °C for 160 s	$T_{(IRSL\ 200\ °C)}$
(9)	Return to step 1 and T = T +20 °C	